

Characterization of the transcriptome, nucleotide sequence polymorphism, and natural selection in the desert adapted mouse *Peromyscus eremicus*

Matthew D. MacManes¹, Michael B. Eisen²,

¹ Department of Molecular, Cellular and Biomedical Sciences, University of New Hampshire, Durham NH, USA

² HHMI and University of California, Berkeley, Berkeley, CA, USA

* E-mail: macmanes@gmail.com, @PeroMHC

1 Abstract

2 As a direct result of intense heat and aridity, deserts are thought to be among the most harsh of
 3 environments, particularly for their mammalian inhabitants. Given that osmoregulation can be
 4 challenging for these animals, with failure resulting in death, strong selection should be observed
 5 on genes related to the maintenance of water and solute balance. One such animal, *Peromyscus*
 6 *eremicus*, is native to the desert regions of the southwest United States and may live its entire
 7 life without oral fluid intake. As a first step toward understanding the genetics that underlie
 8 this phenotype, we present a characterization of the *P. eremicus* transcriptome. We assay four
 9 tissues (kidney, liver, brain, testes) from a single individual and supplement this with popu-
 10 lation level renal transcriptome sequencing from 15 additional animals. We identified a set of
 11 transcripts undergoing both purifying and balancing selection based on estimates of Tajima's
 12 D. In addition, we used the branch-site test to identify a transcript -Slc2a9, likely related to
 13 desert osmoregulation – undergoing enhanced selection in *P. eremicus* relative to a set of related
 14 non-desert rodents.

15

16 Introduction

17 Deserts are widely considered one of the harshest environments on Earth. Animals living in
 18 desert environments are forced to endure intense heat and drought, and as a result, species liv-
 19 ing in these environments are likely to possess specialized mechanisms to deal with them. While
 20 living in deserts likely involves a large number of adaptive traits, the ability to osmoregulate –
 21 to maintain the proper water and electrolyte balance – appears to be paramount [1]. Indeed,
 22 the maintenance of water balance is one of the most important physiologic processes for all
 23 organisms, whether they be desert inhabitants or not. Most animals are exquisitely sensitive
 24 to changes in osmolality, with slight derangement eliciting physiologic compromise. When the
 25 loss of water exceeds dietary intake, dehydration - and in extreme cases, death - can occur.

Thus there has likely been strong selection for mechanisms supporting optimal osmoregulation in species that live where water is limited. Understanding these mechanisms will significantly enhance our understanding of the physiologic processes underlying osmoregulation in extreme environments, which will have implications for studies of human health, conservation, and climate change.

The genes and structures responsible for the maintenance of water and electrolyte balance are well characterized in model organisms such as mice [2], rats [3–5], and humans [6–8]. These studies, many of which have been enabled by newer sequencing technologies, provide a foundation for studies of renal genomics in non-model organisms. Because researchers have long been interested in desert adaptation, a number of studies have looked at the morphology or expression of single genes in the renal tissues of desert adapted rodents *Phyllotis darwini* [9], *Psammomys obesus* [10], and *Perognathus penicillatus* [11]. More recently, full renal transcriptomes have been generated for *Dipodomys spectabilis* and *Chaetodipus baileyi*, [12] as well as *Abrothrix olivacea* [13].

These studies provide a rich context for current and future work aimed at developing a synthetic understanding of the genetic and genomic underpinnings of desert adaptation in rodents. As a first step, we have sequenced, assembled, and characterized the transcriptome (using four tissue types - liver, kidney, testes and brain) of a desert adapted cricetid rodent endemic to the southwest United States [14], *Peromyscus eremicus*. These animals have a lifespan typical of small mammals, and therefore an individual may live its entire life without ever drinking water. These rodents have distinct advantage over other desert animals (e.g. *Dipodomys*) in that they breed readily in captivity, which enables future laboratory studies of the phenotype of interest. In addition, the focal species is positioned in a clade of well known animals (e.g. *P. californicus*, *P. maniculatus*, and *P. polionotus*) [15] with growing genetic and genomic resources [16–18]. Together, this suggests that future comparative studies are possible.

While the elucidation of the mechanisms underlying adaptation to desert survival is beyond the scope of this manuscript, we aim to lay the groundwork by characterizing the transcriptome from four distinct tissues (brain, liver, kidney, testes). These data will be included in the current larger effort aimed at sequencing the entire genome. Further, via sequencing the renal tissue of a total of 15 additional animals, we characterize nucleotide polymorphism and genome-wide patterns of natural selection. Together, these investigations will aid in our overarching goal to understand the genetic basis of adaptation to deserts in *P. eremicus*.

61 **Materials and Methods**

62 **Animal Collection and Study Design**

63 To begin to understand how genes may underlie desert adaptation, we collected 16 individuals
 64 from a single population of *P. eremicus* over a two-year time period (2012-2013). These individ-
 65 uals were captured in live traps and then euthanized using isoflurane overdose and decapitation.
 66 Immediately post-mortem, the abdominal and pelvic organs were removed, cut in half (in the
 67 case of the kidneys), placed in RNAlater and flash frozen in liquid nitrogen. Removal of the
 68 brain, with similar preservation techniques, followed. Time from euthanasia to removal of all
 69 organs never exceeded five minutes. Samples were transferred to a -80C freezer at a later date.
 70 These procedures were approved by the Animal Care and Use Committee located at the Univer-
 71 sity of California Berkeley (protocol number R224) and University of New Hampshire (protocol
 72 number 130902) as well as the California Department of Fish and Game (protocol SC-008135)
 73 and followed guidelines established by the American Society of Mammalogy for the use of wild
 74 animals in research [19].

75 **RNA extraction and Sequencing**

76 Total RNA was extracted from each tissue using a TRIzol extraction (Invitrogen) following the
 77 manufacturer’s instructions. Because preparation of an RNA library suitable for sequencing is
 78 dependent on having high quality, intact RNA, a small aliquot of each total RNA extract was
 79 analyzed on a Bioanalyzer 2100 (Agilent, Palo Alto, CA, USA). Following confirmation of sample
 80 quality, the reference sequencing libraries were made using the TruSeq stranded RNA prep kit
 81 (Illumina), while an unstranded TruSeq kit was used to construct the other sequencing libraries.
 82 A unique index was ligated to each sample to allow for multiplexed sequencing. Reference
 83 libraries (n=4 tissue types) were then pooled to contain equimolar quantities of each individual
 84 library and submitted for Illumina sequencing using two lanes of 150nt paired end sequencing
 85 employing the rapid-mode of the HiSeq 2500 sequencer at The Hubbard Center for Genome
 86 Sciences (University of New Hampshire). The remaining 15 libraries were similarly multiplexed
 87 and sequenced in a mixture of 100nt paired and single end sequencing runs across several lanes
 88 of an Illumina HiSeq 2000 at the Vincent G. Coates Genome Center (University of California,
 89 Berkeley).

90 **Sequence Data Preprocessing and Assembly**

91 The raw sequence reads corresponding to the four tissue types were error corrected using the
 92 software *bless* version 0.17 [20] using *kmer*=25, based on the developer’s default recommenda-
 93 tions. The error-corrected sequence reads were adapter and quality trimmed following recom-

mendations from MacManes [21] and Mbandi [22]. Specifically, adapter sequence contamination and low quality nucleotides (defined as PHRED <2) were removed using the program Trimmomatic version 0.32 [23]. Reads from each tissue were assembled using the Trinity version released 17 July 2014 [24]. We used flags to indicate the stranded nature of sequencing reads and set the maximum allowable physical distance between read pairs to 999nt. The assembly was conducted on a linux workstation with 64 cores and 512Gb RAM. To filter the raw sequence assembly, we downloaded *Mus musculus* cDNA and ncRNA datasets from Ensembl (ftp://ftp.ensembl.org/pub/release-75/fasta/mus_musculus/) and the *Peromyscus maniculatus* reference transcriptome from NCBI (ftp://ftp.ncbi.nlm.nih.gov/genomes/Peromyscus_maniculatus_bairdii/RNA/). We used a blastN (version 2.2.29+) procedure (default settings, evalset to 10^{-10}) to identify contigs in the *P. eremicus* dataset likely to be biological in origin. This procedure, when a reference dataset is available, retains more putative transcripts than a strategy employing expression-based filtering (remove if TMP <1 [25]) of the raw assembly. We then concatenated the filtered assemblies from each tissue into a single file and reduced redundancy using the software cd-hit-est version 4.6 [26] using default settings, except that sequences were clustered based on 95% sequence similarity. This multi-fasta file was used for all subsequent analyses, including annotation and mapping.

Assembled Sequence Annotation

The filtered assemblies were annotated using the default settings of the blastN algorithm [27] against the Ensembl cDNA and ncRNA datasets described above, downloaded on 1 August 2014. Among other things, the Ensemble transcript identifiers were used in the analysis of gene ontology conducted in the PANTHER package [28]. Next, because rapidly evolving nucleotide sequences may evade detection by blast algorithms, we used HMMER3 version 3.1b1 [29] to search for conserved protein domains contained in the dataset using the Pfam database [30]. Lastly, we extracted putative coding sequences using Transdecoder version 4Jul2014 (<http://transdecoder.sourceforge.net/>)

To identify patterns of gene expression unique to each tissue type, we mapped sequence reads from each tissue type to the reference assembly using bwa-mem (version cloned from Github 7/1/2014) [31]. We estimated expression for the four tissues individually using default settings of the software eXpress version 1.51 [32]. Interesting patterns of expression, including instances where expression was limited to a single tissue type, were identified and visualized.

Population Genomics

In addition to the reference individual sequenced at four different tissue types, we sequenced 15 other conspecific individuals from the same population in Palm Desert, California. Sequence data were mapped to the reference transcriptome using bwa-mem. The alignments were sorted and converted to BAM format, then passed to the program ANGSD version 0.610, which was used for calculating the folded site frequency spectrum (SFS) and Tajima's D [33].

Natural Selection

To characterize natural selection on several genes related to water and ion homeostasis, we identified several of the transcripts identified as experiencing positive selection in a recent work on desert-adaptor *Dipodomys* rodents. The coding sequences corresponding to these genes, Solute Carrier family 2 member 9 (Slc2a9) and the Vitamin D3 receptor (Vdr), were extracted from the dataset, aligned using the software MACSE version 1.01b [34] to homologous sequences in *Mus musculus*, *Rattus norvegicus*, *Peromyscus maniculatus*, and *Homo sapiens* as identified by the conditional reciprocal best blast procedure (CRBB, [35]). An unrooted gene tree was constructed using the online resource Clustal-Omega, and the tree and alignment were analyzed using the branch-site model (model=2, nsSites=2, fix_omega=0 versus model=2, nsSites=2, fix_omega=1, omega=1) implemented in PAML version 4.8 [36,37]. Significance was evaluated via the use of the likelihood ratio test.

Results and Discussion

RNA extraction, Sequencing, Assembly, Mapping

RNA was extracted from the hypothalamus, renal medulla, testes, and liver from each individual using sterile technique. TRIzol extraction resulted in a large amount of high quality (RIN \geq 8) total RNA, which was then used as input. Libraries were constructed as per the standard Illumina protocol and sequenced as described above. The number of reads per library varied from 56 million strand-specific paired-end reads in Peer360 kidney, to 9 million single-end reads in Peer321 (Table 1, available on the Short Read Archive accession XXX). Adapter sequence contamination and low-quality nucleotides were eliminated, which resulted in a loss of $<2\%$ of the total number of reads. These trimmed reads served as input for all downstream analyses.

Table 1

DATASET	NUM. RAW READS	SRA ACCESSION
PEER360 TESTES	32M PE/SS	SRR1575398
PEER360 LIVER	53M PE /SS	SRR1575397
PEER360 KIDNEY	56M PE/SS	SRR1575396
PEER360 BRAIN	23M PE/SS	SRR1575395
PEER305	19M PE	SRR1575434
PEER308	15M PE	SRR1575437
PEER319	14M PE	SRR1575439
PEER321	9M SE	SRR1575441
PEER340	16M PE	SRR1575443
PEER352	14M PE	SRR1575464
PEER354	9M SE	SRR1575466
PEER359	14M PE	SRR1575492
PEER365	16M PE	SRR1575493
PEER366	16M PE	
PEER368	14M PE	SRR1575624
PEER369	14M PE	SRR1575625
PEER372	17M SE	
PEER373	23M SE	
PEER380	16M SE	
PEER382	14M SE	

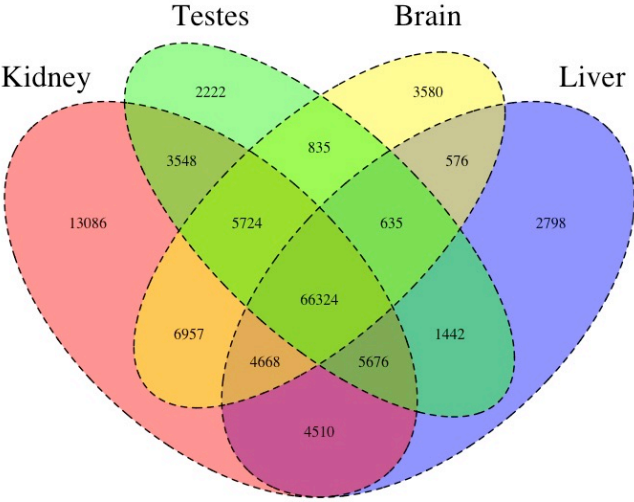
Table 1. The number of sequencing reads per sample, indicated by Peer[number]. PE=paired end, SS=strand specific, SE=single end sequencing.

Transcriptome assembly for each tissue type was accomplished using the program Trinity [24]. The raw assembly for brain, liver, testes, and kidney contained 185425, 222096, 180233, and 514091 assembled sequences respectively. This assembly was filtered using a blastN procedure against the *Mus* cDNA and ncRNA and *P. maniculatus* cDNAs, which resulted in a final dataset containing 68331 brain-specific transcripts, 71041 liver-specific transcripts, 67340 testes-specific transcripts, and 113050 kidney-specific transcripts. Mapping the error-corrected adapter/quality trimmed reads to these datasets resulted in mapping 94.98% (87.01% properly paired) of the brain-derived reads to the brain transcriptome, 96.07% (88.13% properly paired) of the liver-derived reads to the liver transcriptome, 96.81% (85.10% properly paired) of the testes-derived reads to the testes transcriptome, and 91.87% (83.77% properly paired) of the kidney-derived reads to the kidney transcriptome. Together, these statistics suggest that the tissue-specific transcriptomes are of extremely high quality. All tissue-specific assemblies are to be made available on Dryad, and until then are stored on Dropbox

176)https://www.dropbox.com/sh/2jwzd8p6n6eluco/AAA03nSdXb_u4wtQZRTwqW9ia?dl=0).

177

178 **Figure 1**



179

180 Figure 1. The Venn Diagram.

181 We then estimated gene expression on each of these tissue-specific datasets, which allowed
182 us to understand expression patterns in the multiple tissues (Pero.tissue.xprs, will be made
183 available on Dryad, until then on Dropbox ([https://www.dropbox.com/sh/2jwzd8p6n6eluco/](https://www.dropbox.com/sh/2jwzd8p6n6eluco/AAA03nSdXb_u4wtQZRTwqW9ia?dl=0)
184 [AAA03nSdXb_u4wtQZRTwqW9ia?dl=0](https://www.dropbox.com/sh/2jwzd8p6n6eluco/AAA03nSdXb_u4wtQZRTwqW9ia?dl=0))). Specifically, we constructed a Venn diagram (Figure 1)
185 that allowed us to visualize the proportion of genes whose expression was limited to a single
186 tissue and those whose expression was ubiquitous. 66324 transcripts are expressed on all tissue
187 types, while 13086 are uniquely expressed in the kidney, 2222 in the testes, 3580 in the brain,
188 and 2798 in the liver. The kidney appears to an outlier in the number of unique sequences,
189 though this could be the result of the recovery of more lowly expressed transcripts that may be
190 the result of deeper sequencing.

191

192 In addition to this, we estimated mean TMP (number of transcripts per million) for all tran-
193 scripts. Table 2 consists of the 10 genes whose mean TMP was the highest. Several genes in this
194 list are predominately present in a single tissue type. For instance Transcript_126459, Albumin
195 is very highly expressed in the liver, but less so in the other tissues. It should be noted, however,
196 that making inference based on uncorrected values for TPM is not warranted. Statistical testing
197 for differential expression was not implemented due to the fact that no replicates are available.

198

After expression estimation, the filtered assemblies were concatenated together, and after the removal of redundancy with cd-hit-est, 123,123 putative transcripts remained (to be made available on Genbank, and until then are stored on Dropbox https://www.dropbox.com/sh/2jwzd8p6n6eluco/AAA03nSdXb_u4wtQZRTwqW9ia?dl=0). From this filtered concatenated dataset, we extracted 71626 putative coding sequences (72Mb, to be made available on Dryad). Of these 71626 sequences, 38221 were complete exons (containing both start and stop codons), while the others were either truncated at the 5-prime end (20239 sequences), the 3-prime end (6445 sequences), or were internal (6721 sequencing with neither stop nor start codon). The results of a Pfam search conducted on the predicted amino acid sequences will be found on Dryad, and until then are stored on Dropbox https://www.dropbox.com/sh/2jwzd8p6n6eluco/AAA03nSdXb_u4wtQZRTwqW9ia?dl=0.

Table 2

Transcript ID	Testes	Liver	Kidney	Brain	Genbank ID	Gene ID
Transcript_83842	2.05E+03	6.40E+03	1.03E+04	5.47E+03	DQ073446.1	COX2
Transcript_126459	1.43E+01	2.22E+04	2.77E+01	6.73E+00	XM.006991665.1	Alb
Transcript_128937	4.39E+00	1.91E+04	4.74E+02	2.23E+00	XM.007627625.1	Apoa2
Transcript_81233	1.71E+03	5.23E+03	6.11E+03	3.08E+03	XM.006993867.1	Fth1
Transcript_94125	3.67E+01	1.08E+04	2.09E+03	2.75E+00	XM.006977178.1	CytP450
Transcript_119945	5.03E+03	1.15E+03	1.33E+03	3.71E+03	XM.008686011.1	Ubb
Transcript_5977	4.95E+00	1.01E+04	3.05E+02	3.58E+02	XM.006978668.1	Tf
Transcript_4057	2.62E+01	9.32E+03	1.34E+02	8.38E+01	XM.006994871.1	Apoc1
Transcript_112523	4.07E+02	7.36E+03	7.78E+02	9.54E+02	XM.006994872.1	Apoe
Transcript_98376	1.98E+00	8.66E+03	1.02E+00	2.68E+00	XM.006970208.1	Ttr

Table 2. The 10 transcripts with the highest mean TPM (transcripts per million).

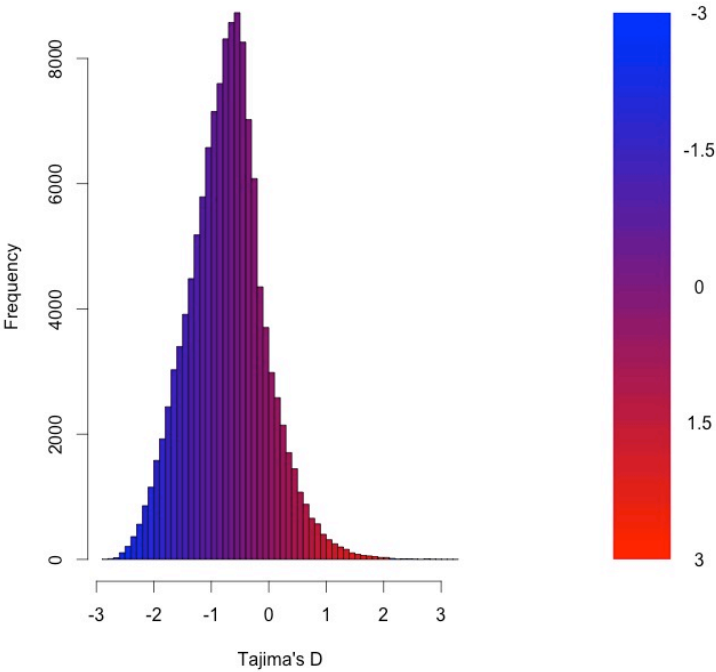
Population Genomics

As detailed above, RNAseq data from 15 individuals were mapped to the reference transcriptome with the resulting BAM files being used as input to the software package ANGSD. The Tajima's D statistic was calculated for all transcripts covered by at least 14 of the 15 individuals. In brief, a negative Tajima's D - a result of lower than expected average heterozygosity - is often associated with purifying or directional selection, recent selective sweep or population bottleneck. In contrast, a positive value for Tajima's D represents higher than expected average heterozygosity, often associated with balancing selection.

224 The distribution of the estimates of Tajima's D for all of the assembled transcripts is shown
225 in Figure 2. The distribution is skewed toward negative values (mean=-0.89, variance=0.58),
226 which is likely the result of purifying selection, a model of evolution commonly invoked for
227 coding DNA sequences [38]. Table 3 presents the 10 transcripts whose estimate of Tajima's D
228 is the greatest, while Table 4 presents the 10 transcripts whose estimate of Tajima's D is the
229 least. The former list of genes is likely to contain transcripts experiencing balancing selection
230 in the studied population. This list includes, interestingly, genes obviously related to solute
231 and water balance (e.g. *Clcnkb* and a transmembrane protein gene) and immune function (a
232 interferon-inducible GTPase and a Class 1 MHC gene). The latter group, containing transcripts
233 whose estimates of Tajima's D are the smallest are likely experiencing purifying selection. Many
234 of these transcripts are involved in core regulatory functions where mutation may have strongly
235 negative fitness consequences.

236

237 **Figure 2**



238

239 Figure 2. The distribution of Tajima's D for all putative transcripts.

240 **Table 3**

241

Transcript ID	GenBank ID	Description	Tajima's D
Transcript_49049	XM.006533884.1	heterogeneous nuclear ribonucleoprotein H1 (HnrnpH1)	3.26
Transcript_38378	XM.006522973.1	Son DNA binding protein (Son)	3.19
Transcript_126187	NM.133739.2	transmembrane protein 123 (Tmem123)	3.02
Transcript_70953	XM.006539066.1	chloride channel Kb (Clcnkb)	2.96
Transcript_37736	XM.006997718.1	h-2 class I histocompatibility antigen	2.92
Transcript_21448	XM.006986148.1	zinc finger protein 624-like	2.84
Transcript_47450	NM.009560.2	zinc finger protein 60 (Zfp60)	2.82
Transcript_122250	XM.006539068.1	chloride channel Kb (Clcnkb)	2.81
Transcript_78367	XM.006496814.1	CDC42 binding protein kinase alpha (Cdc42bpa)	2.78
Transcript_96470	XM.006987129.1	interferon-inducible GTPase 1-like	2.77

Table 3. The 10 transcripts with the highest values for Tajima's D, which suggests balancing selection.

244 **Table 4**

245

Transcript ID	GenBank ID	Description	Tajima's D
Transcript_84359	XM.006991127.1	nuclear receptor coactivator 3 (Ncoa3)	-2.82
Transcript_87121	XM.006970128.1	methyl-CpG binding domain protein 2 (Mbd2)	-2.82
Transcript_125755	EU053203.1	alpha globin gene cluster	-2.78
Transcript_87128	XM.006976644.1	membrane-associated ring finger (March5)	-2.76
Transcript_55468	XM.006978377.1	Vpr binding protein (Vprbp)	-2.75
Transcript_116042	XM.006980811.1	membrane associated guanylate kinase (Magi3)	-2.75
Transcript_18966	XM.006982814.1	ubiquitin protein ligase E3 component n-recognin 5 (Ubr5)	-2.75
Transcript_122204	XM.008772511.1	zinc finger protein 612 (Zfp612)	-2.75
Transcript_100550	XM.006971297.1	bromodomain adjacent to zinc finger domain, 1B (Baz1b)	-2.74
Transcript_33267	XM.006975561.1	pumilio RNA-binding family member 1 (Pum1)	-2.75

Table 4. The 10 transcripts with the lowest values for Tajima's D, which suggests purifying or directional selection.

248 Natural Selection

249 To begin to test the hypothesis that selection on transcripts related to osmoregulation is en-
 250 hanced in the desert adapted *P. eremicus*, we implemented the branch-site test as described
 251 above by setting the sequence corresponding to *P. eremicus* for both Slc2a9 and Vdr as the

foreground lineages in 2 distinct program executions. These two transcripts were chosen specifically because they - the former significantly - were recently linked to osmoregulation in a desert rodent [12]. The test for *Slc2a9* was highly significant ($2\Delta L_{nl}=51.4$, $df=1$, $p=0$), indicating enhanced selection in *P. eremicus* relative to the other lineages. The branch site test for positive selection conducted on the *Vdr* gene was non-significant ($2\Delta L_{nl}=0.68$, $df=1$, $p=1$). This limited analysis of selection is to be followed up by an analysis of genome wide patterns of natural selection.

Conclusions

As a direct result of intense heat and aridity, deserts are thought to be amongst the harshest environments, particularly for mammalian inhabitants. Given that osmoregulation can be challenging for these animals - with failure resulting in death - strong selection should be observed on genes related to the maintenance of water and solute balance. This study aimed to characterize the transcriptome of a desert-adapted rodent species, *P. eremicus*. Specifically, we characterized the transcriptome of four tissue types (liver, kidney, brain, and testes) from a single individual and supplemented this with population-level renal transcriptome sequencing from 15 additional animals. We identified a set of transcripts undergoing both purifying and balancing selection based on Tajima's D. In addition, we used a branch site test to identify a transcript, likely related to desert osmoregulation, undergoing enhanced selection in *P. eremicus* relative to a set of non-desert rodents.

Acknowledgments

References

1. Walsberg G (2000) Small mammals in hot deserts: Some generalizations revisited. *Bio-science* 50: 109–120.
2. Tatum R, Zhang Y, Salleng K, Lu Z, Lin JJ, et al. (2009) Renal salt wasting and chronic dehydration in claudin-7-deficient mice. *Renal Physiology* 298: F24–F34.
3. Romero DG, Plonczynski MW, Welsh BL, Gomez-Sanchez CE, Zhou MY, et al. (2007) Gene expression profile in rat adrenal zona glomerulosa cells stimulated with aldosterone secretagogues. *Physiological Genomics* 32: 117–127.

- 282 4. Rojek A, Rojek A, Fuchtbauer E, Fuchtbauer E, Kwon T, et al. (2006) Severe urinary
283 concentrating defect in renal collecting duct-selective AQP2 conditional-knockout mice.
284 PNAS 103: 6037–6042.
- 285 5. Nielsen S, Chou C, Marples D, Christensen E, Kishore B, et al. (1995) Vasopressin
286 increases water permeability of kidney collecting duct by inducing translocation of
287 aquaporin-CD water channels to plasma-membrane. PNAS 92: 1013–1017.
- 288 6. Mobasheri A, Marples D, Young IS, Floyd RV, Moskaluk CA, et al. (2007) Distribution
289 of the AQP4 Water Channel in Normal Human Tissues: Protein and Tissue Microarrays
290 Reveal Expression in Several New Anatomical Locations, including the Prostate Gland
291 Seminal Vesicles. Channels 1: 30–39.
- 292 7. Bedford JJ, Leader JP, Walker RJ (2003) Aquaporin expression in normal human kidney
293 and in renal disease. Journal of the American Society of Nephrology 14: 2581–2587.
- 294 8. Nielsen S, Kwon TH, Christensen BM, Promeneur D, Frøkiaer J, et al. (1999) Physiology
295 and pathophysiology of renal aquaporins. Journal of the American Society of Nephrology
296 10: 647–663.
- 297 9. Gallardo PA, Cortés A, Bozinovic F (2005) Phenotypic flexibility at the molecular and
298 organismal level allows desert-dwelling rodents to cope with seasonal water availability.
299 Physiological and Biochemical Zoology 78: 145–152.
- 300 10. Kaissling B, De Rouffignac C, Barrett JM, Kriz W (1975) The structural organization
301 of the kidney of the desert rodent *Psammomys obesus*. Anatomy and Embryology 148:
302 121–143.
- 303 11. Altschuler EM, Nagle RB, Braun EJ, Lindstedt SL, Krutzsch PH (1979) Morphological
304 study of the desert heteromyid kidney with emphasis on the genus *Perognathus*. The
305 Anatomical Record 194: 461–468.
- 306 12. Marra NJ, Romero A, DeWoody JA (2014) Natural selection and the genetic basis of
307 osmoregulation in heteromyid rodents as revealed by RNA-seq. Molecular Ecology 23:
308 2699–2711.
- 309 13. Giorello FM, Feijoo M, D’Elía G, Valdez L, Opazo JC, et al. (2014) Characterization of
310 the kidney transcriptome of the South American olive mouse *Abrothrix olivacea*. BMC
311 Genomics 15: 446.
- 312 14. Veal R, Caire W (2001) *Peromyscus eremicus*. Mammalian Species 118: 1–6.

- 313 15. Feng BJ, Sun LD, Soltani-Arabshahi R, Bowcock AM, Nair RP, et al. (2007) Toward
314 a Molecular Phylogeny for *Peromyscus*: Evidence from Mitochondrial Cytochrome- b
315 Sequences. *Journal of Mammalogy* 88: 1146–1159.
- 316 16. Shorter KR, Owen A, anderson V, Hall-South AC, Hayford S, et al. (2014) Natural genetic
317 variation underlying differences in *Peromyscus* repetitive and social/aggressive behaviors.
318 *Behavior genetics* 44: 126–135.
- 319 17. Panhuis TM, Broitman-Maduro G, Uhrig J, Maduro M, Reznick DN (2011) Analysis of
320 Expressed Sequence Tags from the Placenta of the Live-Bearing Fish *Poeciliopsis* (Poe-
321 ciliidae). *Journal of Heredity* 102: 352–361.
- 322 18. Shorter KR, Crossland JP, Webb D, Szalai G, Felder MR, et al. (2012) *Peromyscus* as a
323 Mammalian Epigenetic Model. *Genetics Research International* 2012: 1–11.
- 324 19. Sikes RS, Gannon WL, Animal Care and Use Committee of the American Society of
325 Mammalogists (2011) Guidelines of the American Society of Mammalogists for the use of
326 wild mammals in research. *Journal of Mammalogy* 92: 235–253.
- 327 20. Heo Y, Wu XL, Chen D, Ma J, Hwu WM (2014) BLESS: Bloom filter-based error correc-
328 tion solution for high-throughput sequencing reads. *Bioinformatics* 30: 1354–1362.
- 329 21. MacManes MD (2014) On the optimal trimming of high-throughput mRNA sequence
330 data. *Frontiers in Genetics* 5.
- 331 22. Mbandi SK, Hesse U, Rees DJG, Christoffels A (2014) A glance at quality score: Impli-
332 cation for *de novo* transcriptome reconstruction of Illumina reads. *Frontiers in Genetics*
333 5: 17.
- 334 23. Lohse M, Bolger AM, Nagel A, Fernie AR, Lunn JE, et al. (2012) RobiNA: A user-friendly,
335 integrated software solution for RNA-Seq-based transcriptomics. *Nucleic Acids Research*
336 40: W622–7.
- 337 24. Haas BJ, Papanicolaou A, Yassour M, Grabherr M, Blood PD, et al. (2013) *De novo*
338 transcript sequence reconstruction from RNA-seq using the Trinity platform for reference
339 generation and analysis. *Nature Protocols* 8: 1494–1512.
- 340 25. **MacManes** MD, Lacey EA (2012) The Social Brain: Transcriptome Assembly and Char-
341 acterization of the Hippocampus from a Social Subterranean Rodent, the Colonial Tuco-
342 Tuco (*Ctenomys sociabilis*). *PLOS ONE* 7: e45524.

- 343 26. Li W, Godzik A (2006) Cd-hit: A fast program for clustering and comparing large sets of
344 protein or nucleotide sequences. *Bioinformatics* 22: 1658–1659.
- 345 27. Camacho C, Coulouris G, Avagyan V, Ma N, Papadopoulos J, et al. (2009) BLAST+:
346 architecture and applications. *BMC Bioinformatics* 10: 421.
- 347 28. Mi H (2004) The PANTHER database of protein families, subfamilies, functions and
348 pathways. *Nucleic Acids Research* 33: D284–D288.
- 349 29. Wheeler TJ, Eddy SR (2013) nhmmer: DNA homology search with profile HMMs. *Bioin-*
350 *formatics* 29: 2487–2489.
- 351 30. Punta M, Coghill PC, Eberhardt RY, Mistry J, Tate J, et al. (2012) The Pfam protein
352 families database. *Nucleic Acids Research* 40: D290–301.
- 353 31. Li H (2013) Aligning sequence reads, clone sequences and assembly contigs with BWA-
354 MEM. *arXivorg* .
- 355 32. Roberts A, Pachter L (2013) Streaming fragment assignment for real-time analysis of
356 sequencing experiments. *Nature Methods* 10: 71–73.
- 357 33. Korneliussen I Thorfinn Sand Moltke, Albrechtsen a, Nielsen R (2013) Calculation of
358 Tajima’s D and other neutrality test statistics from low depth next-generation sequencing
359 data. *BMC Bioinformatics* 14: 289.
- 360 34. Ranwez V, Harispe S, Delsuc F, Douzery EJP (2011) MACSE: Multiple Alignment of
361 Coding SEquences Accounting for Frameshifts and Stop Codons. *PLOS ONE* 6: e22594.
- 362 35. Aubry S, Kelly S, Kämpers BMC, Smith-Unna RD, Hibberd JM (2014) Deep Evolutionary
363 Comparison of Gene Expression Identifies Parallel Recruitment of Trans-Factors in Two
364 Independent Origins of C4 Photosynthesis. *PLOS Genetics* 10: e1004365.
- 365 36. Yang Z, dos Reis M (2011) Statistical Properties of the Branch-Site Test of Positive
366 Selection. *Molecular Biology and Evolution* 28: 1217–1228.
- 367 37. Yang Z (2007) PAML 4: Phylogenetic Analysis by Maximum Likelihood. *Molecular*
368 *Biology and Evolution* 24: 1586–1591.
- 369 38. Chamary JV, Parmley JL, Hurst LD (2006) Hearing silence: non-neutral evolution at
370 synonymous sites in mammals. *Nature Reviews Genetics* 7: 98–108.